Scientific Research Publishing

Advances in Aerospace Science and Technology, 2024, 9, 148-166
https://www.scirp.org/journal/aast
ISSN Online: 2473-6724
ISSN Print: 2473-6708

Study on Flow Characteristics and Performance of Baffled Shock Two-Dimensional Vector Nozzle

Masum Hossain*, Yasir Kamal, Sourav Mallick, Md Rifat Jahan Angkon

Department of Aeronautical Engineering, Nanchang Hangkong University, Nanchang, China
Email: *hossainmasum1999@gmail.com

How to cite this paper: Hossain, M., Kamal, Y., Mallick, S. and Angkon, M.R.J. (2024) Study on Flow Characteristics and Performance of Baffled Shock Two-Dimensional Vector Nozzle. *Advances in Aerospace Science and Technology*, **9**, 148-166.
https://doi.org/10.4236/aast.2024.94012

Received: September 6, 2024
Accepted: December 16, 2024
Published: December 19, 2024

Abstract

This research paper presents a numerical study on the flow characteristics and performance of a baffled shock two-dimensional vector nozzle. The baffled shock vector nozzle is a type of fluid thrust vectoring nozzle that uses a secondary injection to deflect the primary flow and generate a vector angle. The fluid thrust vectoring technology is regarded as a key technology for the development of very low detectable vehicles because of its advantages, such as fast response, lightweight, and good stealth performance. The main objectives of this study are to investigate the effects of various parameters such as slot interval distance, slot width, injection angle, nozzle pressure ratio, secondary flow pressure ratio, and outflow Mach number on the deflection angle, thrust coefficient, thrust efficiency, and secondary flow ratio of the nozzle. The numerical simulations are carried out using the k-epsilon turbulence model, which is validated by comparing it with experimental data. The results indicate that optimizing the slot interval distance and width, increasing the injection angle, adjusting the nozzle pressure ratio and secondary flow pressure ratio, and controlling the outflow Mach number can enhance the nozzle performance. The results also reveal the complex flow phenomena inside the nozzle, such as shock wave interactions, flow separation and reattachment, and boundary layer effects. The study provides a comprehensive understanding of the flow characteristics and performance of a baffled shock two-dimensional vector nozzle and offers some guidance for its design and optimization.

Keywords

Thrust Vector Control, Baffle Displacement, The Opening of Discharge Gap, The Thrust Vector Angle, Thrust Coefficient

1. Introduction

The development of supersonic and hypersonic aircraft is a strategic and visionary goal for future aerospace technology, with great symbolic and driving effects [1]-[3]. Modern aerospace technology has advanced in recent years, and various types of aircraft need to meet higher performance standards, such as super-maneuverability, supersonic cruise, short/vertical take-off and landing, stealth performance, etc. Thrust vectoring control (TVC) is one of the essential technologies for this purpose [4]. Thrust vectoring control technology means that the propulsion system can not only generate forward thrust for the aircraft but also change the direction of the engine thrust and create a pitch, yaw, roll control force, and moment simultaneously or separately, which can directly control the aircraft's attitude or replace some of the control surface functions, achieve maneuvers, or high angle of attack flight that are impossible or even stalled for the original aircraft [5]-[7]. In supersonic and hypersonic aircraft, the nozzle transforms the thermal energy of high-temperature gas from the combustion chamber into kinetic energy, thus producing thrust to support the aircraft's flight [8]-[10]. Thrust vectoring control has to be implemented in the engine exhaust system, so the thrust vectoring nozzle as a core component has become a focus of vector control research. As national military power plays an increasingly important role in the development of exchange and cooperation and security and stability, high-efficiency thrust vectoring nozzle technology that can enhance the maneuverability and stability of supersonic and hypersonic aircraft has always been a hot research topic for major military-industrial powers in the world.

Since the 1970s, major developed countries such as Europe and America have started to research and develop thrust vectoring nozzles for use on fighter jets on a large scale. Thrust vectoring nozzles are installed on the U.S. military's F-22, F-35, Russian military's MiG-1.44, Su-37, and Britain's "Harrier" fighter jets, which greatly enhance the performance of fighter jets.

There are two kinds of nozzles that can change the direction of the thrust: mechanical and fluid. Mechanical nozzles [11] have parts like gas rudders, spoilers or spherical plates that move the fluid inside the nozzle to change the thrust direction; fluid nozzle does not have any moving parts in the nozzle but use flow control methods to change and control how the mainstream of the engine nozzle flows and deflects, which changes the thrust direction.

There are five main structural schemes for mechanical thrust vector nozzles [12]: jet vane thrust vector nozzle (PV, Puckering Victory), two-dimensional contracting distending vector nozzle (2DCD, 2-Dimensional Contracting Distending), pitch-type asymmetric vector nozzle, spherical convergent flap nozzle (SCFN, Spherical Convergent Flap Nozzle) and axial-symmetric vectoring exhaust nozzle (AVEN, Axial-Symmetric Vectoring Exhaust Nozzle).

Jet vane thrust vector nozzle (PV): A jet vane vector nozzle is a thrust vector control by installing multiple jet vanes on the engine nozzle or the tail of the aircraft. The X-31 verification machine with a jet vane thrust vector nozzle. The

thrust vector is generated by controlling the action of the jet vanes, thereby changing the direction of the jet flow. The vector nozzle has a simple structure, less modification and low cost for the original engine, and is easy to install on the existing aircraft. However, since the jet vanes are installed outside the nozzle, they are greatly affected by the external flow during the work process of producing the vector effect, and the size, weight, drag and radar reflection area are also increased. A type of vector nozzle inserts a baffle into the tail jet of the engine nozzle, causing the boundary layer separation upstream of the baffle to form an oblique shock wave, and the undisturbed main flow in the nozzle deflects relative to the nozzle axis through the oblique shock wave to generate a thrust with vector effect.

Two-dimensional contracting distending vector nozzle (2DCD): The two-dimensional contracting distending vector nozzle (2DCD), is to use the up and down rotation of the upper and lower plate-shaped components installed at the end of the engine tail nozzle to achieve changing the direction of the exhaust gas flow. The thrust vector nozzle with this structure has a flat rear contour size, which greatly reduces the drag of the rear fuselage. The disadvantage is that the structure is heavy, and in the case of a single engine, it can only provide a pitch moment and cannot provide a yaw moment.

Spherical convergent flap nozzle [13] (SCFN): The spherical convergent flap nozzle (SCFN) has a spherical convergent section and a rectangular expansion section. The convergent section rotates, driving the nozzle to swing left and right, generating yaw thrust; in the expansion section, the flap swings up and down to produce pitch thrust. The nozzle's throat area and nozzle area can work independently or in a specific proportional relationship, and the rotation is flexible; the rectangular nozzle has good stealth performance; advanced brush seals are used between the convergent section and the spherical shell, and the side walls use honeycomb seals, which have good sealing performance. However, there are also some drawbacks to this structure. Although a spherical structure is used, the manipulation actuation system still cannot be designed too small, which easily increases the weight; in the convergent section, that is, before the throat section of the subsonic section rotates, the aerodynamic load is large; under multi-axis conditions, at least another set of control actuation cylinders is required, and the thrust vector system structure becomes more complicated; the axial rotation length is large so that the contour size is large and the external resistance increases.

Pitch-type axisymmetric vector nozzle [14]: The pitch-type axisymmetric vector nozzle divides the cylindrical section of the nozzle into two sections and sets two axial pins on both sides of the connection so that the nozzle can swing up and down in the pitch plane. The thrust vector nozzle with this method has a simple movement principle and can be directly added to the original axisymmetric contracting distending nozzle without changing it. The disadvantage is that the length of the rotating section is long, generally 1.3 - 1.7 m, and the rotating section is forward, the external resistance is large, and the structural load received by the attachment is large.

Axial-symmetric vectoring exhaust nozzle (AVEN): is a device that can produce thrust vectoring by deflecting the nozzle's convergent and divergent sections within a certain range and can rotate 360 degrees. Thrust vectoring is the ability to change the direction of the thrust produced by a jet engine, which can improve the maneuverability and agility of a fighter aircraft. AVEN is considered to be the main nozzle form of the fifth-generation fighter, but it also has some challenges, such as fluid-solid-thermal coupling problems.

There are five main methods to achieve thrust vectoring by fluid control: shock vectoring method (SVC, Shock Vectoring Control), throat offset method (TS, Throat Skewing), dual throat method (DTN, Dual Throat Nozzle), co-flow method (Co-Flow), and counter-flow method (Counter-Flow).

Shock vectoring control (SVC): Shock vectoring control (SVC) is a method of injecting a high-pressure secondary flow into the supersonic region of the nozzle expansion section. The high-pressure secondary flow interferes with the main flow to form a shock wave, and the direction of the gas flow changes after the shock wave to form a vector effect of thrust. A high-pressure secondary flow can only produce a vector thrust in one direction, and the interaction and coordination of multiple high-pressure secondary flows can produce vector thrusts in different directions. And the vector angle increases with the increase of shock wave intensity. The advantage of shock vectoring control is that it can produce relatively large vector angles and high vector efficiency, but in order to achieve gas flow deflection through shock wave action in the supersonic region, it requires the nozzle to work in an over-expanded state, so shock vectoring control also has shock wave loss and over-expansion. The thrust loss is caused by expansion, and its thrust coefficient is generally between 0.86 and 0.94.

Throat offset method (TS): The throat offset method (TS) is a method of injecting a secondary flow near the throat of the nozzle, controlling the position of the sonic surface to change the direction of the main flow in the nozzle. Since the secondary flow is injected at the throat of the nozzle, the shock wave is avoided, and there is no flow loss caused by the shock wave, so the thrust coefficient of the nozzle using this thrust vectoring method is generally larger than that of the nozzle using the shock vectoring method, but correspondingly this method also has the disadvantage of small thrust vectoring angle. The throat offset method (TS) makes the gas flow in the nozzle tilt under the condition of an asymmetric jet, achieving the effect of thrust vectoring. When a symmetric secondary flow is injected at the throat of the nozzle, there will be no thrust vectoring effect, but due to the effect of the secondary flow, a new fluid throat is formed in the nozzle, changing the throat area, and making the thrust, exit Mach number and other nozzle performance parameters have a certain degree of change. Therefore, the secondary flow can achieve throat adjustment (nozzle thrust adjustment) and thrust vectoring adjustment, respectively, by symmetric and asymmetric injection methods.

Double throat method (DTN): The double throat method (DTN) is designed to solve the problem of small thrust vectoring angle produced by the throat offset

method. It is based on the configuration of the throat offset method and adds a convergent section to the nozzle. The deflection effect produced by the throat offset method is amplified by the flow separation in the cavity formed by the concave structure. By controlling the degree of flow separation in the cavity, different vector angles are obtained. The double throat method, like the throat offset method, avoids the shock wave loss caused by the shock wave generation and, at the same time, increases the convergent section, making the gas flow expand and accelerate outside the nozzle, reducing the flow loss caused by over-expansion, and improving the thrust coefficient of the nozzle. However, because this method introduces secondary flow in the nozzle throat and increases the convergent section, the flow easily stagnates, reducing the nozzle flow coefficient.

Co-directional secondary flow method (Co-Flow): The co-directional flow method (Co-Flow) is based on the Coanda effect [15]. The Coanda effect refers to the tendency of fluids to leave their original direction of flow and follow the surface of a protruding object. The structural feature of the nozzle using this method is to install Coanda surfaces symmetrically on the upper and lower sides of the nozzle outlet and inject a thin layer of high-speed gas flow along the tangential direction, forming a low-pressure area on the Coanda surface, thus attracting high-pressure main flow deflection. However, this method can only achieve good control efficiency when the main flow velocity is low subsonic. When the nozzle pressure drop ratio (NPR) is large, and the main flow velocity is high, this thrust vectoring method fails.

Reverse secondary flow method (Counter-Flow): The reverse secondary flow method adds a jacket downstream of the nozzle outlet section, forming a channel for reverse flow. When the main flow needs to be deflected, the vacuum pump suction system starts to form a negative pressure, which deflects the main gas flow and produces a lateral force. When a negative pressure difference is generated in the upper cavity, the main flow deflects upward, and when a negative pressure difference is generated in the lower cavity, the main flow deflects downward. Because it is to control the jet in the tangential direction, it has the characteristics of small thrust loss, and the thrust coefficient is about 0.92 - 0.97, which is considered to be a promising control method. However, because this method adds a jacket to the nozzle outlet, the large trailing edge plate and the fuselage are difficult to integrate, and the existence of the vacuum pump also increases the overall weight. More seriously, when the main flow has a large deflection angle, due to the Coanda effect, the flow easily adheres to the control surface, resulting in a sudden change in thrust direction and bringing risks to flight control.

A baffle is a device that creates oblique shock waves to slow down and compress supersonic airflow. A baffle can be used in a CD nozzle to control the exit pressure and the mass flow rate of the fluid.

The baffled shock of the nozzle could mean one of two things:

The condition when oblique shock waves are generated by a baffle inside a CD nozzle to match the exit pressure with the back pressure and achieve supersonic

flow outside the nozzle. This condition is also called under expanded nozzle [16].

One example is a converging-diverging nozzle that is used to accelerate a fluid to supersonic speeds. Depending on the pressure difference between the upstream and downstream regions, the nozzle can produce different types of shock waves inside or outside the nozzle. For example:

If the back pressure is too low, oblique shock waves will be generated by the nozzle exit, and the flow outside the nozzle will be supersonic. This is called an under expanded nozzle [17] [18].

Another example is a baffled nozzle that has a device inside the nozzle that creates oblique shock waves to control the exit pressure and the mass flow rate of the fluid. This can be used to achieve supersonic flow outside the nozzle without over expanding or under expanding the nozzle.

The thrust vectoring nozzle first appeared in Britain, causing great panic. Since 1987, NASA has conducted technical research on the F/A-18 HARV high-angle-of-attack validation aircraft. Three gas rudders were installed at the nozzle exit of the F-404 engine to adjust the deflection of the mainstream, thus providing pitch and yaw forces for the aircraft to enhance maneuverability at high angles of attack. Finally, a controllable flight attack angle of nearly 70˚ was achieved on the validation aircraft [18].

Subsequently, the United States and Germany jointly designed an enhanced validation aircraft for X-31, which also carried three gas rudders at the engine outlet, achieving a deflection of the engine mainstream in the pitch and yaw directions relative to the engine axis ± 10˚ [19] [20].

Since the 1960s, Hollstein H J and Eatough R G [21]-[25] have conducted a series of cold gas jet and gas jet flap-type shock wave thrust vector control experiments. They obtained the influence laws of flap parameters such as flap position and shape on thrust vector, laying the theoretical foundation for flap engineering application. Through numerical simulation of RANS equations, Kozic *et al.* obtained the flow field characteristics of a two-dimensional flap-type shock wave thrust vector nozzle and applied it to the design of a two-dimensional flap thrust vector nozzle. The design of the flap-type shock wave thrust vector nozzle is unique, and currently, this method has only been applied to the Russian R-73 missile and its derivative models.

In 1973, P&W proposed a plan for a binary nozzle thrust vector, which had the functions of providing pitch thrust, reverse thrust, and adjusting the throat area. It also completed the verification in wind tunnel tests. Subsequently, flight tests were completed using F-15S/MTD (Short Take Off and Landing/Maneuver Technology Demonstrator), which shortened the take-off and landing distances by 30% and 40%, respectively. In 2014, Japan's fifth-generation fighter ATD-X with a binary vector nozzle XF3-400 engine showed that Japan had mastered this thrust vector technology.

In the 1980s, a new type of thrust vector nozzle-spherical convergent adjustment flap vector jet nozzle (SCFN) was successfully developed by P&W. The nozzle has

yaw, pitch and reverse thrust capabilities, and a full-size SCFN model test was conducted on the XTE-65 demonstrator in 1994. The results showed that the nozzle performance was excellent, weighing about 60% of the binary vector nozzle mounted on F-22/F119, and achieving ± 20˚ of pitch/yaw angle. The reverse thrust efficiency can reach 60% - 65% under non-after-burning conditions.

The asymmetric thrust vector nozzle is developed based on the asymmetric variable convergent-divergent nozzle, and the addition of the thrust deflection structure and control system enables the entire nozzle to deflect within the circumferential range, achieving thrust vector control. The two American companies GE and P&W have respectively carried out long-term research on this, and the typical research results are the AVEN nozzle mounted on the F-110-GE-100 engine and the P/YBBN nozzle mounted on the F-100-PW-229, respectively. These two asymmetric vector nozzles have undergone ground and air tests and finally reached a high level of technical maturity [26]-[30].

The authors aim to verify the effects of key parameters, such as slot interval, slot width, injection angle, nozzle pressure ratio, secondary flow pressure ratio, and Mach number, on the performance of a baffled shock vector nozzle. These parameters are analyzed in terms of their impact on deflection angle, thrust coefficient, thrust efficiency, and secondary flow ratio. The study also seeks to understand complex flow dynamics within the nozzle, including shock wave interactions, flow separation, and boundary layer effects. Additionally, the authors validate the accuracy of the k-ε turbulence model by comparing the simulation results with experimental data. Ultimately, the research provides insights to guide the design and optimization of baffled shock vector nozzles for improved performance.

2. Control Equation and Physical Model

2.1. System of Governing Equation

Navies-Stokes (N-S) equation is a governing differential equation that describes the flow of continuous fluid medium, taking into account the fluid viscosity, heat transfer, etc., based on the conservation of mass, momentum and energy. The numerical simulation study in this paper ignores body force and radiation heat transfer. The general form of N-S equation is:

$$\frac{\partial \boldsymbol{U}}{\partial t}+\frac{\partial \boldsymbol{F}_c}{\partial x}+\frac{\partial \boldsymbol{G}_c}{\partial y}+\frac{\partial \boldsymbol{H}_D}{\partial z}=\frac{\partial \boldsymbol{F}_D}{\partial x}+\frac{\partial \boldsymbol{G}_D}{\partial y}+\frac{\partial \boldsymbol{H}_D}{\partial z} \tag{1}$$

where, $\boldsymbol{U}$ is the conservative variable vector1, $\boldsymbol{F}_c$, $\boldsymbol{G}_c$, $\boldsymbol{H}_c$ are the convection flux vectors, $\boldsymbol{F}_D$, $\boldsymbol{G}_D$, $\boldsymbol{H}_D$ are the viscous diffusion flux vectors. The expressions are:

$$\boldsymbol{U}=\begin{bmatrix}\rho\\ \rho u\\ \rho v\\ \rho w\\ 0\end{bmatrix},\ \boldsymbol{F}_c=\begin{bmatrix}\rho u\\ \rho u^2+p\\ \rho vu\\ \rho wu\\ up\end{bmatrix},\ \boldsymbol{G}_c=\begin{bmatrix}\rho v\\ \rho uv+p\\ \rho v^2\\ \rho wv\\ vp\end{bmatrix},\ \boldsymbol{H}_c=\begin{bmatrix}\rho w\\ \rho uw\\ \rho vw\\ \rho w^2+p\\ wp\end{bmatrix} \tag{2}$$

$$\boldsymbol{F}_D = \begin{bmatrix} 0 \\ \sigma_{xx} \\ \sigma_{yx} \\ \sigma_{zx} \\ u\sigma_{xx} + v\sigma_{yx} + w\sigma_{zx} \end{bmatrix}, \boldsymbol{G}_D = \begin{bmatrix} 0 \\ \sigma_{xy} \\ \sigma_{yy} \\ \sigma_{zy} \\ u\sigma_{xy} + v\sigma_{yy} + w\sigma_{zy} \end{bmatrix}, \boldsymbol{H}_D = \begin{bmatrix} 0 \\ \sigma_{xz} \\ \sigma_{yz} \\ \sigma_{zz} \\ u\sigma_{xz} + v\sigma_{yz} + w\sigma_{zz} \end{bmatrix} \quad (3)$$

In the viscous diffusion flux vector, the stress expression is:

$$\sigma_{xy} = \sigma_{yx} = \mu\left(\frac{\partial v}{\partial x} + \frac{\partial u}{\partial y}\right), \ \sigma_{yz} = \sigma_{zy} = \mu\left(\frac{\partial w}{\partial y} + \frac{\partial v}{\partial z}\right), \ \sigma_{zx} = \sigma_{xz} = \mu\left(\frac{\partial u}{\partial z} + \frac{\partial w}{\partial x}\right) \quad (4)$$

$$\sigma_{xx} = \frac{2}{3}\mu\left(2\frac{\partial u}{\partial x} - \frac{\partial v}{\partial y} - \frac{\partial w}{\partial z}\right), \ \sigma_{yy} = \frac{2}{3}\mu\left(2\frac{\partial v}{\partial y} - \frac{\partial u}{\partial x} - \frac{\partial w}{\partial z}\right), \ \sigma_{zz} = \frac{2}{3}\mu\left(2\frac{\partial w}{\partial z} - \frac{\partial u}{\partial x} - \frac{\partial v}{\partial y}\right) \quad (5)$$

In the above formula, ρ is the density of the gas, u, v, w are the velocity components along the coordinate axes x, y, z, p is the gas pressure and is the dynamic viscosity coefficient.

2.2. Physical Model and Computational Domain

Given the design nozzle expansion ratio of 7, the exit radius of 70.00 mm, and the specific values of the profile parameters arc throat radius ratio, contraction ratio, contraction section length ratio, expansion section length ratio, expansion angle and exit half angle. At this time, the nozzle throat radius, inlet radius and contraction and expansion section lengths can be calculated from the above data. The detailed data of the nozzle profile parameters are shown in Table 1.

Table 1. Nozzle profile parameters and values.

Parameters	Value
Expansion Ration (ε)	7
Shrinkage Ration (n)	3
Expansion Angle ($\theta°$)	30
Exit Half Angle ($\varphi°$)	5
Laryngeal Radius (R_T)	10.00 mm
Nozzle Inlet Radius (R_0)	30.00 mm
Length of Nozzle Shrinkage (L)	40.00 mm
Nozzle Expansion Section Length (L_n)	96.00 mm

Baffle type shock vector nozzle (as shown in Figure 1) is a nozzle that has different baffle heights H on the upper half of the nozzle outlet and different leakage gap openings on the lower half of the nozzle wall. The nozzle blockage ratio C is the ratio of the baffle height H to the nozzle exit height H_O. The leakage gap opening k is the axial width of the leakage gap. The nozzle blockage ratio C is the ratio of the baffle height H to the nozzle exit radius R_e, that is, $C = \frac{H}{R_e}$.

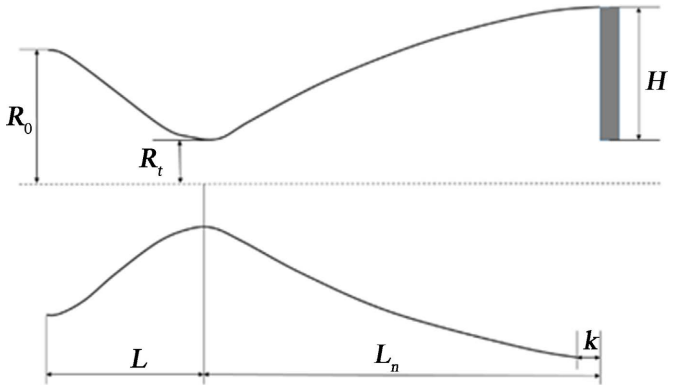

Figure 1. Baffle type shock vector nozzle.

2.3. Calculation Method

Solve the Reynolds time averaged N-S equation, using the Standard k-ε model for turbulence. The baseline two-transport-equation model solving for k and ε. This is the default k-ε model. Coefficients are empirically derived and valid for fully turbulent flows only. Options to account for viscous heating, buoyancy, and compressibility are shared with other k-ε models. Widely used despite the known limitations of the model. Performs poorly for complex flows involving severe pressure gradient, separation, and strong streamline curvature. Suitable for initial iterations, initial screening of alternative designs, and parametric studies. The study's reliance on the k-ε turbulence model introduces several potential limitations that could affect the accuracy and generalizability of the results. While the k-ε model is widely used for its computational efficiency and robustness in simulating high-Reynolds-number flows, it has known drawbacks, particularly when dealing with complex flow phenomena like shock-wave boundary layer interactions, flow separation, and reattachment. The model's assumptions may oversimplify turbulence behavior, leading to inaccuracies in predicting localized flow structures and shock interactions critical for nozzle performance.

Specifically, the k-ε model struggles with capturing anisotropic turbulence and may over-predict or under-predict flow separation zones, which are key to understanding thrust efficiency and shock wave dynamics. This limitation could impact the study's ability to provide precise guidance for real-world applications, especially under extreme conditions or for highly optimized designs. Alternative turbulence models, such as Reynolds Stress Models (RSM) or Large Eddy Simulation (LES), though computationally expensive, might yield more accurate insights for such cases.

From a computational perspective, constraints such as mesh resolution, convergence criteria, and computational time also pose challenges. A fine mesh is required to accurately resolve the small-scale flow structures, particularly near walls and shocks, but this increases computational demand significantly. Trade-offs between computational cost and accuracy may limit the scope of parameter exploration or the fidelity of results, potentially overlooking subtle but important effects.

Addressing these limitations would involve either validating the findings against experimental data more extensively or incorporating more advanced numerical

methods and turbulence models to enhance the reliability and generalizability of the results.

3. Boundary Conditions and Calculation Method

3.1. Meshing and Boundary Condition

The grid divisions baffle-type shock wave vector nozzle model respectively. In the process of grid division, dense boundary layer grids are set to more accurately predict the fluid flow separation near the nozzle wall and other situations. The grid is divided separately at the baffle and discharge gap of the nozzle, which is convenient for setting different working conditions, and the grid is refined to ensure the accuracy of the calculation results.

The fluid shock wave vector nozzle is a secondary flow nozzle set on the upper wall of the basic nozzle, and different fluid shock wave vector nozzles are formed by changing the geometric parameters of the secondary flow nozzle. In the process of grid division, the position of the secondary flow nozzle and the wall of the nozzle is encrypted to facilitate the study of the fluid flow characteristics in the nozzle and ensure the accuracy of the calculation results. When the geometric parameters of the secondary flow nozzle of the fluid shock wave vector nozzle change, the model needs to be reconstructed and divided into grids.

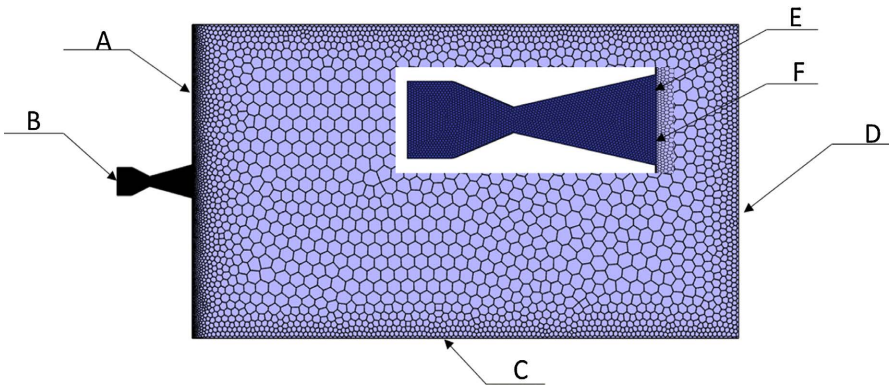

Figure 2. Grid division of baffle-type shock wave vector nozzle model.

The calculation model and its grid division are shown in Figure 2. The grid is finely divided in the nozzle, and where the flow parameters have large gradients to ensure the accuracy of the calculation results. B is the inlet of the nozzle set as a pressure inlet, A is the inlet of the external flow field set as a pressure inlet, C is the far-field boundary of the external flow field, D is the outlet of the external flow field set as a pressure outlet, E is the baffle of the nozzle, set as a solid wall, F is the discharge gap of the nozzle, which communicates with the external flow field and is fixed as an internal flow condition.

3.2. Boundary Conditions and Initialization

Boundary conditions should be defined sensibly to protect the precision of

simulation calculation results and prevent divergence of the calculation process.

Following is the setting of the boundary conditions for the fluid shock wave nodes and baffle shock vector nodes model calculations.

The entire pressure P_n is applied to Nozzle Inlet A under the pressure inlet condition. Set according to various NPR, total temperature T_n is 300 K; inlet B adopts pressure far-field circumstances, total pressure is set to 101,502 Pa, and total temperature T_s is 300 K; total inlet pressure P_s at secondary intake G is set according to different SPR, total temperature T_s is 300 K; and inlet C adopts pressure far-field conditions, total pressure is set to 101,502 Pa. The total pressure is set to a standard atmospheric pressure (101,325 Pa), and the total temperature is set to 300 K. The outlet boundary D adopts the pressure outlet boundary. The static pressure, static temperature, and Mach number of the incoming flow, together with flow velocity and direction, are provided at the far-field boundary C of the external flow field, which adopts the far-field boundary conditions. Because of the nozzle's symmetry, just half of it is investigated in order to minimize the number of calculation grids and streamline the computation. Therefore, the symmetric boundary condition sets the plane of symmetry F. The model's walls have an adiabatic no-slip boundary condition. Due to the requirement to alter the opening and shutting of the baffle and the discharge gap, the baffle E and the discharge gap F are configured as adiabatic no-slip boundary conditions or interior planes, depending on the requirements of the working circumstances. The initialization of the model computation uses the usual initialization, and the entire process is altered in accordance with the nozzle's pressure inlet boundary condition. Initialization of the computational model.

4. Results and Discussion

4.1. Vector Nozzle Performance Evaluation Index

A basic task of TVC system design is to generate a vector thrust of required strength and duration. Optimal performance of the system is achieved when thrust in the desired direction is produced with minimal losses. Therefore, this paper regards the thrust vector angle and thrust coefficient as the main evaluation indexes of TVC system performance.

The principle of the baffle-type thrust vector control is shown in Figure 3. A baffle is inserted as an obstacle in the supersonic gas flow, an oblique shock wave is generated upstream of it, a high-pressure recirculation zone is generated, and the pressure in the recirculation zone is redistributed. Additional pressure is generated on the pipe wall, which tilts the direction of thrust. The thrust vector

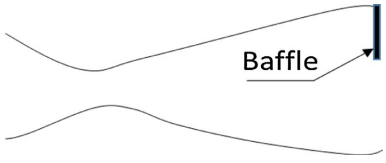

Figure 3. Schematic diagram of baffle thrust vector control principle.

angle and the magnitude of the thrust mainly depend on the pressure redistribution in the recirculation zone and the change in the direction and magnitude of the gas outflow.

By examining the axial and radial directions, the thrust formula can be obtained as:

$$\begin{cases} T_x = \dot{m}V_{ex} + \left(P_e - P_a\right)A_e \\ T_y = \dot{m}V_{ey} \end{cases} \tag{6}$$

In the formula: $\dot{m}$ is the mass flow rate, V_{ei} is the average velocity of each direction on the nozzle exit plane, P_e is the average static pressure on the nozzle exit plane, P_a is the ambient pressure, A_e is the gas flow area of the nozzle exit. The thrust vector angle T_x can be calculated by the axial thrust T_y and the radial thrust δ.

$$\delta = \arctan\frac{T_y}{T_x} \tag{7}$$

The performance of the nozzle is measured by the thrust coefficient:

$$C_f = \frac{\sqrt{T_x^2 + T_y^2}}{T_i} \tag{8}$$

Among them is the isentropic derivation:

$$T_i = \dot{W}_n\sqrt{\frac{2\gamma}{\gamma-1}RT_t^*\left[1-\left(\frac{1}{R_{np}}\right)\right]^{\frac{\gamma-1}{\gamma}}} \tag{9}$$

Among them, $\dot{W}_n$ is the mainstream flow rate of the nozzle; γ is the specific heat ratio of the gas, and the value here is 1.4; R is the gas constant, and the value is 287 J/(kg·K); T_t^* is the total temperature; R_{np} is the drop pressure ratio under the design state of the nozzle.

4.2. The Effect of Blockage Ratio on the Performance of Flap-Type Shock Vector Nozzle

The existence of the baffle is the reason for the oblique shock wave generation in the baffle-type shock wave vector nozzle. When there is no leakage gap, the effect of the blockage ratio on the nozzle performance under different pressure drop ratios (NPR = 10, 15, 20, 25) is studied, where the blockage ratio C = 0, 0.25, 0.5, 0.75, 1.0 has a total of 5 working conditions.

Figure 4 shows the Mach number cloud map of several working conditions. It can be seen from the figure that as the blockage ratio increases, the jet deflection angle of the nozzle tail flow increases significantly, but it decreases when the blockage ratio reaches 1.0. As the blockage ratio increases, the oblique shock wave is gradually restricted in the nozzle, and the high-pressure backflow area also increases. As the blockage ratio increases further, when the oblique shock wave is completely restricted in the nozzle, the thrust vector angle of the nozzle reaches its maximum. But when the blockage ratio increases again, the oblique shock

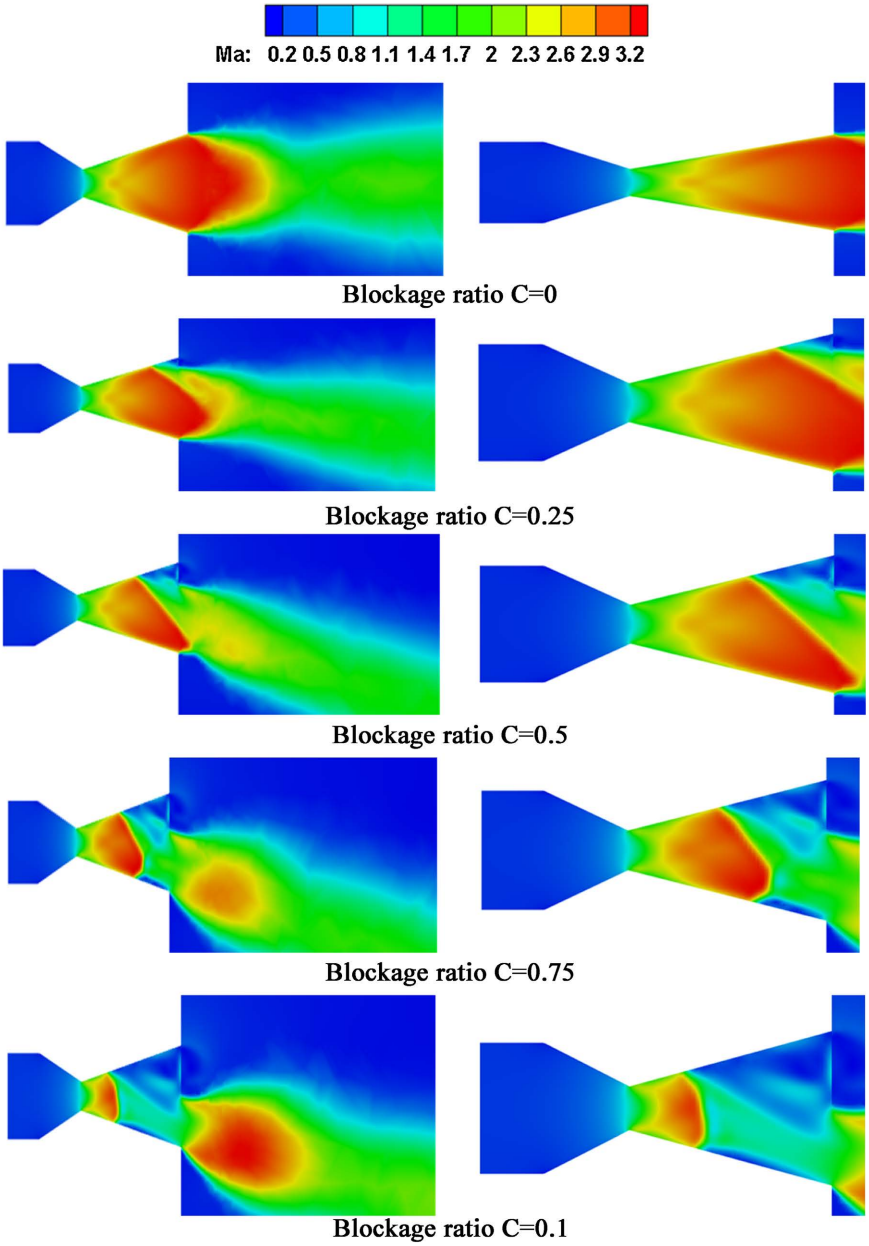

Figure 4. Mach number distribution cloud map of nozzle under different blockage ratios.

wave will develop in the direction of the nozzle throat, as shown in the cloud map when $C = 1.0$. At this time, the oblique shock wave is no longer a free shock wave but is restricted in the nozzle by the influence of the lower wall of the nozzle and interacts with the boundary layer on the lower wall of the nozzle, causing flow separation near the lower wall of the nozzle, forming a separation shock wave in the mainstream of the nozzle. The separation shock wave intersects with the oblique shock wave and produces a reflected shock wave, forming a complex shock wave system inside the nozzle. It is precisely because of the influence of the complex shock wave system that under small blockage ratios, the stable pressure on the lower wall of the nozzle increases locally, the pressure difference between

the upper and lower walls of the nozzle decreases, and the thrust vector angle of the nozzle also decreases significantly.

The injection angle enhances thrust efficiency by controlling how the secondary flow interacts with the primary flow, directly affecting shock wave formation and flow dynamics within the nozzle. An optimized injection angle ensures the secondary flow deflects the primary flow effectively, minimizing turbulence and flow separation while maintaining smooth mixing. This reduces energy losses caused by shock-induced pressure drops and chaotic interactions. Additionally, the injection angle influences the positioning and strength of oblique shock waves, ensuring they direct the flow efficiently while minimizing disturbances in the boundary layer. By optimizing these interactions, the nozzle achieves better conversion of thermal energy into directional momentum, improving thrust vectoring performance and overall efficiency.

Optimizing the slot interval and width can improve nozzle performance, but there are potential trade-offs and limitations to consider. Modifying these parameters beyond optimal values could lead to diminishing returns or practical issues. For instance, excessively increasing the slot interval may weaken the interaction between the secondary and primary flows, reducing the deflection angle and thrust vectoring effectiveness. On the other hand, decreasing the slot interval too much could result in higher flow resistance, increased turbulence, or structural complexity, which may compromise efficiency. Similarly, while increasing the slot width can enhance the flow rate of secondary injection and improve thrust deflection, it may also require a higher secondary flow pressure ratio, which could increase energy consumption and reduce overall system efficiency. Additionally, excessively wide slots might disrupt the balance of shock wave interactions, leading to unstable flow patterns or increased flow separation. These trade-offs highlight the importance of finding a balanced design that maximizes performance while minimizing losses or complications.

Figure 5 is the thrust vector angle change line with nozzle pressure ratio (NPR). As we see in the graph, the thrust vector angle decreases with different nozzle pressure ratios. It happens because of the use of different blockages in the nozzle, which we call baffles. Figure 6 and Figure 7 are the thrust coefficient and thrust vector angle with NPR and shade ratio. It has changed the lines with the NPR and shade ratio, respectively. Figure 8 is the thrust vectoring coefficient with shade ratio. As the shade ratio increases, the thrust coefficient increases, and the thrust vector angle decreases. It can be seen that NPR increases, the thrust angle decreases, and the thrust coefficient increases.

Shock wave interactions significantly influence thrust efficiency in baffled shock vector nozzles by affecting energy transfer and flow dynamics. These interactions can cause energy losses due to pressure drops and turbulence, particularly when oblique or normal shocks form within the nozzle. Additionally, shock-induced flow separation along the nozzle walls can create low-pressure recirculation zones, disrupting smooth flow and reducing the efficiency of momentum

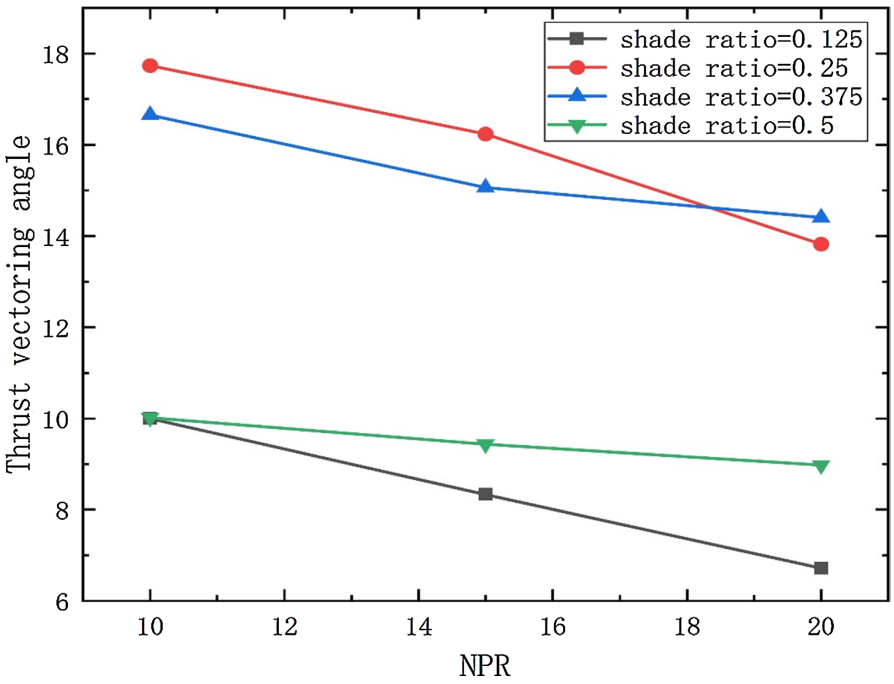

Figure 5. Thrust vectoring angle vs NPR.

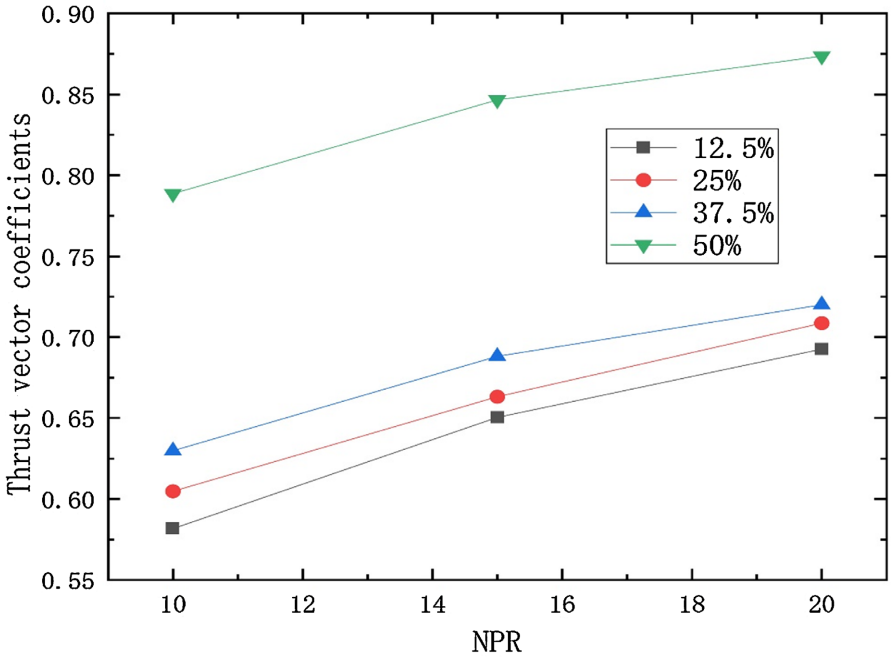

Figure 6. Thrust vectoring coefficients vs NPR.

transfer. Misaligned or overly strong shocks may also lead to over-expansion or under-expansion of the flow, further lowering thrust efficiency. Moreover, the interaction between secondary injection and shock waves alters the shock structure, impacting deflection angles and the effective contribution of secondary flow to thrust. Optimizing these shock interactions is crucial for achieving maximum thrust efficiency and overall nozzle performance.

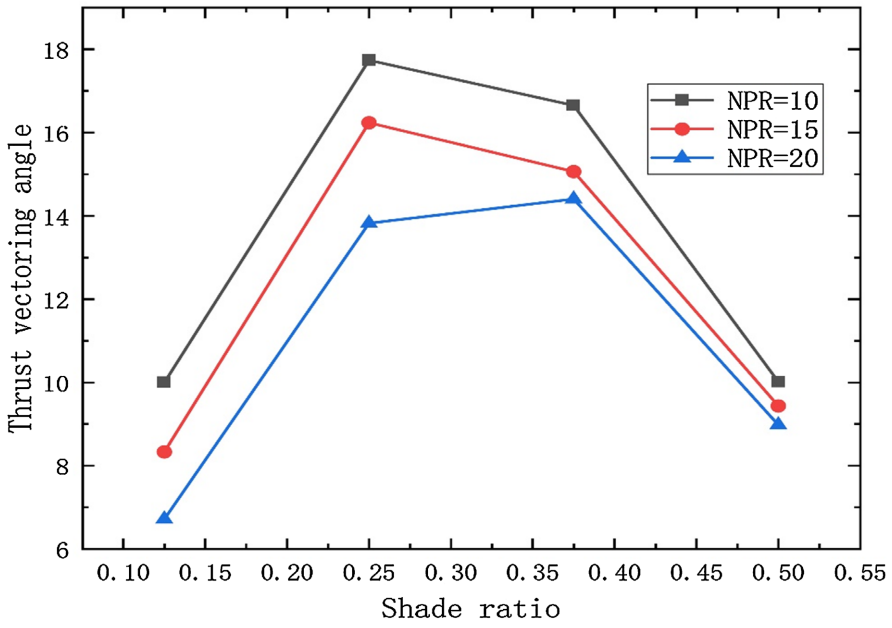

Figure 7. Thrust vector angle vs shade ratio.

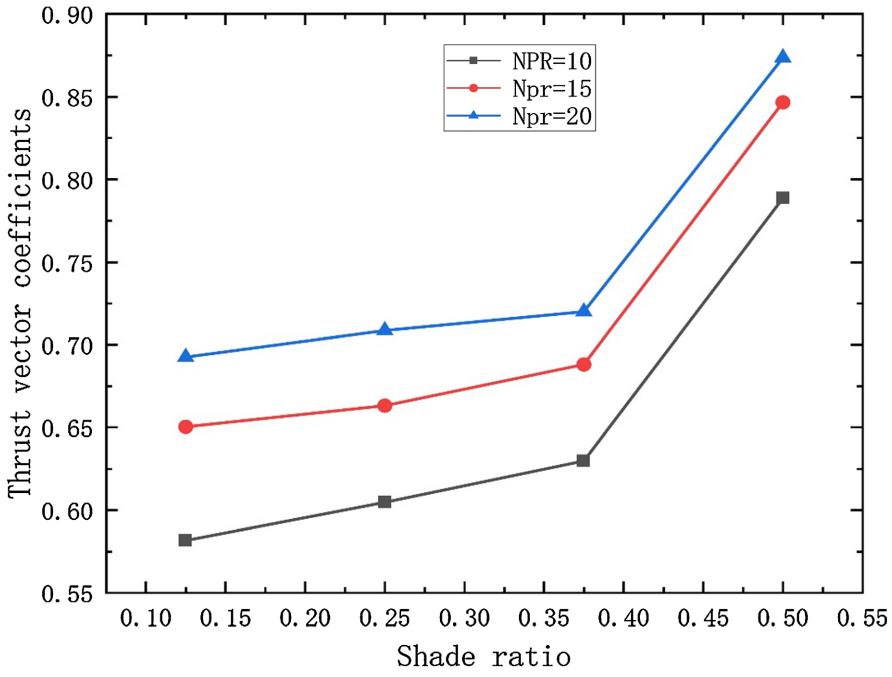

Figure 8. Thrust vectoring coefficients vs shade ratio.

The secondary flow pressure ratio (SPR) plays a critical role in the nozzle's performance, as it governs the interaction between the primary and secondary flows, impacting thrust deflection, efficiency, and flow stability. The sensitivity of nozzle performance to changes in SPR depends on how it influences key flow phenomena such as shock wave strength, flow separation, and boundary layer dynamics.

When SPR is too low, the secondary flow may not exert sufficient force to effectively deflect the primary flow, leading to reduced thrust vectoring efficiency

and smaller deflection angles. Conversely, excessively high SPR can introduce strong shock waves and turbulence, resulting in energy losses, potential structural stress on the nozzle, and diminishing returns in terms of performance gains.

In real-world applications, the optimal SPR range is influenced by factors such as the operating conditions of the vehicle (e.g., speed, altitude, and maneuvering requirements) and system energy constraints. For instance, in low-detectable or stealthy vehicles, maintaining a moderate SPR is essential to balance performance with energy efficiency and avoid excessive noise or heat signatures. Fine-tuning the SPR to match mission-specific requirements ensures the nozzle achieves maximum efficiency and reliability under varying conditions.

5. Conclusions

This paper presents a numerical study of the flow characteristics and performance of a two-dimensional shock vector nozzle with baffles. The baffles are used to control the shock wave angle and position in the nozzle, which affects the thrust vectoring and efficiency. The k-epsilon turbulence model is employed to simulate the supersonic flow in the nozzle, and the results are validated by comparing them with experimental data. The effects of baffle geometry, injection parameters, and nozzle pressure ratio on the nozzle performance are analyzed. The results show that the baffles can improve the vector angle and efficiency by adjusting the shock wave structure in the nozzle. The optimal baffle configuration depends on the injection parameters and nozzle pressure ratio. The paper provides a useful reference for the design and optimization of baffled shock vector nozzles. The main contributions of this paper are as follows:

It used turbulence models to predict supersonic flows in a two-dimensional shock vector control nozzle.

It reveals the significant sensitivity of vector angle and efficiency to jet position, thrust coefficient to nozzle pressure ratio, and secondary flow ratio to nozzle pressure ratio.

It identifies the optimal slot interval distance and slot width for both deflection angle and thrust efficiency under some investigated conditions.

It proposes some design guidelines for improving the vector performance without increasing the secondary flow ratio, such as positioning the jet close to the nozzle outlet and adjusting the oblique shock wave to develop near the nozzle outlet.

Conflicts of Interest

The authors declare no conflicts of interest regarding the publication of this paper.

References

[1] Bertin, J.J. and Cummings, R.M. (2006) Critical Hypersonic Aerothermodynamic Phenomena. *Annual Review of Fluid Mechanics*, **38**, 129-157. https://doi.org/10.1146/annurev.fluid.38.050304.092041

[2] Wu, J. (2017) Extention of Hypersonic Ludwieg Tube to Supersonic Wind Tunnel. *Acta Aerodynamica Sinica*, **36**, 480-492.

[3] Taylor, A.A. and Hoffman, J.D. (1974) Design of Maximum Thrust Nozzles for Nonequilibrium Chemically Reacting Flow. *AIAA Journal*, **12**, 1299-1300. https://doi.org/10.2514/3.49481

[4] Wang, S.X. (2018) Structural Characteristics and Development of Geometrically Adjustable Nozzles. *Journal of Sichuan Ordnance*, **39**, 6-13.

[5] Waithe, K. and Deere, K. (2003) An Experimental and Computational Investigation of Multiple Injection Ports in a Convergent-Divergent Nozzle for Fluidic Thrust Vectoring. 21*st AIAA Applied Aerodynamics Conference*, Orlando, 23-26 June 2003, Article No. 1. https://doi.org/10.2514/6.2003-3802

[6] Sun, D.C. and You, X. (2016) Numerical Study of Engine Thrust Vectoring Scheme. *Journal of Propulsion Technology*, **37**, 436-442.

[7] Xiao, Z.Y., Jiang, X., Mou, B., *et al.* (2017) A Review of Research on Fluid Thrust Vectoring Technology. *Experimental Fluid Mechanics*, **31**, 8-15.

[8] Bianchi, D. and Neri, A. (2015) Numerical Simulation of Chemical Erosion in VEGA Launcher Solid Propellant Rocket Motor Nozzles. *Journal of Propulsion and Power*, **34**, 1-17.

[9] Yang, F., Li, Z.H. and Li, J.C. (2020) Research Progress of Solid Rocket Engine Nozzle Profile. *Vacuum*, **57**, 45-52.

[10] Liu, W.Z., Zhang, N.R., Zhang, C.L. and Zhao, Y.Z. (2006) Design and Numerical Calculation of Nozzle Profile of a Certain Type of Solid Rocket Engine. *Chinese Journal of Engineering Design*, **13**, 99-103.

[11] Freepik (2022) Nozzle Vectors & Illustrations for Free Download. https://www.freepik.com/vectors/nozzle

[12] Meng, Q.M. and Li, Q.S. (1994) Overview of Thrust Vector Nozzle and Its Control Technology. *Academic Symposium on Engine Automatic Control of Chinese Society of Aeronautics and Astronautics*, Maryland, 29 June-1 July 1994.

[13] Wang, Y.X. (2006) Jet Engine Axisymmetric Thrust Vector Nozzle. National Defense Industry Press.

[14] Wood, J.M., Hauer, T.A. and Lippmeier, W.C. (1996) Axisymmetric Vectoring Exhaust Nozzle Thermal Shield: CA, CA2065677 A1.

[15] Kim, H., Raghunathan, S., Setoguchi, T. and Matsuo, S. (2000) Experimental and Numerical Studies of Supersonic Coanda Wall Jets. 38*th Aerospace Sciences Meeting and Exhibit*, Saga, 10-13 January 2000. https://doi.org/10.2514/6.2000-814

[16] Adrian, R.J. and Westerweel, J. (2004) Converging Diverging Nozzle. Virginia Tech.

[17] Brennen, E. (2005) Oblique Shock Wave. California Institute of Technology.

[18] Arens, M. (1963) The Shock Position in Overexpanded Nozzles. *The Journal of the Royal Aeronautical Society*, **67**, 268-269. https://doi.org/10.1017/s0368393100078445

[19] Regenie, V., Gatlin, D., Kempel, R., *et al.* (1992) The F-18 High Alpha Research Vehicle. NASA TM-104253.

[20] Young, J. (2013) X31 VECTOR Program Summary. https://www.semanticscholar.org/paper/X31-VECTOR-Program-Summary-Young/d0cc01e5ac9ac0dab81858fdfd4aa9d0b63b3c0b

[21] Ross, H. and Robinson, M. (2006) X-31: An Example of 20 Years of Successful International Cooperation.

[22] Hollstein, H.J. (1965) Jet Tab Thrust Vector Control. *Journal of Spacecraft and*

Rockets, **2**, 927-930. https://doi.org/10.2514/3.28316

[23] Eatough, R. (1971) Jet Tab Thrust Vector Control System Demonstration. 7*th Propulsion Joint Specialist Conference*, Salt Lake City, 14-18 June 1971. https://doi.org/10.2514/6.1971-752

[24] Eatough, R.G. (1996) Improved Jet Tab Thrust Vector Control for the RGM-345C Booster AD 9-13.

[25] Thanigaiarasu, S., Jayaprakash, S., Elangovan, S. and Rathakrishnan, E. (2008) Influence of Tab Geometry and Its Orientation on Under-Expanded Sonic Jets. *Proceedings of the Institution of Mechanical Engineers, Part G: Journal of Aerospace Engineering*, **222**, 331-339. https://doi.org/10.1243/09544100jaero299

[26] Reddy, D., Zaman, K., Steffen, Jr., C., Steffen, Jr., C., Reddy, D. and Zaman, K. (1997) Numerical Modeling of Jet Entrainment for Nozzles Fitted with Delta Tabs. 35*th Aerospace Sciences Meeting and Exhibit*, Reno, 6-9 January 1997. https://doi.org/10.2514/6.1997-709

[27] Zwerneman, W. and Eller, B. (1994). VISTA/F-16 Multi-Axis Thrust Vectoring (MATV) Control Law Design and Evaluation. 19*th Atmospheric Flight Mechanics Conference*, Scottsdale, 1-3 August 1994, 65. https://doi.org/10.2514/6.1994-3513

[28] Orme, J., Hathaway, R. and Ferguson, M. (1998) Initial Flight Test Evaluation of the F-15 Active Axisymmetric Vectoring Nozzle Performance. 34*th AIAA/ASME/SAE/ASEE Joint Propulsion Conference and Exhibit*, Cleveland, 13-15 July 1998. https://doi.org/10.2514/6.1998-3871

[29] Masum, H., Srree, A.T., Kuldeep, S., *et al.* (2023) Design Conceptualization and Computational Analysis of Cryogenic Engine Nozzle 10.37591/JOMM.

[30] Hossain, M. and Hyder, S. (2024) Improve the Aerodynamics Performance of the Wing Using Shark Denticles. *International Journal of Recent Engineering Science*, **11**, 37-43. https://doi.org/10.14445/23497157/ijres-v11i1p106